Journal of proteome research

Article

pubs.acs.org/jpr

Terms of Use

Differential Ion Mobility Spectrometry Coupled to Tandem Mass Spectrometry Enables Targeted Leukemia Antigen Detection

Udara Dharmasiri,[†,§] Samantha L. Isenberg,[‡] Gary L. Glish,[‡] and Paul M. Armistead*[,†]

[†]Lineberger Comprehensive Cancer Center, University of North Carolina at Chapel Hill, 450 West Drive, 21-244, Chapel Hill, North Carolina 27599, United States

[‡]Department of Chemistry, University of North Carolina at Chapel Hill, 320 Caudill Hall, Chapel Hill, North Carolina 27599, United States

Supporting Information

ABSTRACT: Differential ion mobility spectrometry (DIMS) can be used as a filter to remove undesired background ions from reaching the mass spectrometer. The ability to use DIMS as a filter for known analytes makes DIMS coupled to tandem mass spectrometry (DIMS−MS/MS) a promising technique for the detection of cancer antigens that can be predicted by computational algorithms. In experiments using DIMS−MS/MS that were performed without the use of high-performance liquid chromatography (HPLC), a predicted model antigen, GLR (FLSSANEHL), was detected at a concentration of 10 pM (20 amol) in a mixture containing 94 competing model peptide antigens, each at a concentration of 1 μM. Without DIMS filtering, the GLR peptide was undetectable in the mixture even at 100 nM. Again, without using HPLC, DIMS−MS/MS was used to detect 2 of 3 previously characterized antigens produced by the leukemia cell line U937.A2. Because of its sensitivity, a targeted DIMS−MS/MS methodology can likely be used to probe for predicted cancer antigens from cancer cell lines as well as human tumor samples.

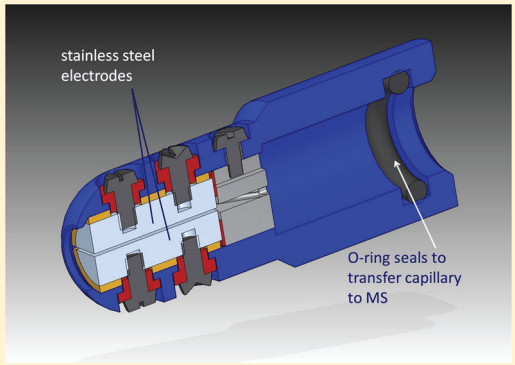

KEYWORDS: *Differential ion mobility spectrometry, DIMS, FAIMS, mass spectrometry, cancer antigen*

INTRODUCTION

Differential ion mobility spectrometry (DIMS) provides a gas-phase separation of ions prior to mass analysis. DIMS has the ability to separate isobaric and isomeric species and therefore can improve the specificity and detection limits of mass spectrometry-based analyses.[1−3] Low electric field ion mobility separations take advantage of the difference in the collisional cross-section of ions, which is directly proportional to the low-field ion mobility.[4,5] At low electric fields the mobility of an ion is independent of the field. However, at high electric fields (>10^4 V/cm), the mobility of an ion becomes dependent on the electric field in a complex function that is still not understood.[4,5] DIMS takes advantage of the change in ion mobility in high electric fields to separate ions based on the difference in ion mobility between low and high electric fields.

Differential ion mobility spectrometers are composed of two parallel electrodes. The gas flow into the mass spectrometer carries ions through the gap between the DIMS electrodes. In "transparent" mode, both of the electrodes are held at the same potential, and all ions are allowed to pass through the device without an ion mobility separation. In "active" mode, an asymmetric waveform is applied to the electrodes. The DIMS waveform alternates between low and high electric fields of opposing polarity, such that the ions zigzag through the device. The $V_{0\text{-}P}$ of the DIMS waveform measured during the high electric field portion is called the dispersion voltage (DV). Because ions have a different mobility in the high field versus low field, they are displaced toward one or the other electrodes during transit through the device. To direct ions of a selected differential ion mobility into the mass spectrometer, a compensation voltage (CV) must be applied to one of the electrodes, which counter balances the displacement due to the differential mobility. Because high-field ion mobility is not yet well understood, the optimum CV and DV for a given analyte are not easily predicted. This makes DIMS currently most useful for targeted analyses, where optimal DIMS conditions for the selection of the analyte of interest can be determined prior to analysis of the real sample. While there is a loss in overall ion signal using DIMS, the background signal (chemical noise) is typically reduced to a much greater extent than the analyte signal because background ions are eliminated through collisions with the DIMS electrodes while target ions are not. The net result is an overall increase in signal-to-noise (S/N).

One potential application for DIMS is the identification of cancer antigens. These antigens consist of a 9−10 amino acid peptide fragment, derived from a cancer associated protein, which is complexed to a class I human leukocyte antigen (HLA) molecule. The peptide/HLA complexes are assembled in the endoplasmic reticulum and subsequently transported to

Received: May 28, 2014
Published: September 3, 2014

and presented on the cancer cell's surface. A cytotoxic $CD8^+$ T-cell expressing a T-cell receptor with high binding affinity for the specific peptide/HLA complex can kill the antigen-presenting cells (i.e., cancer cell) through release of cytotoxic granule proteins.[6−8] Because of the high activity and specificity of cancer-antigen specific CD8+ T-cells and their ability to persist in patients indefinitely, many forms of cancer immunotherapy have been developed to harness this approach in various cancers including melanoma, renal cell carcinoma, prostate cancer, and leukemia.[9−12] The identification of appropriate peptide antigens is a vital part of the development of new T-cell therapies because of the complexity and costs involved with the production and development of these therapeutics and the risks involved with directing T-cells to noncancer (i.e., normal tissue) targets.[13,14]

The majority of cancer antigenic peptides have been confirmed using nontargeted reverse phase high-performance liquid chromatography coupled to tandem mass spectrometry (HPLC−MS) approaches on a complex mixture of antigenic peptides obtained from a cellular sample.[15−20] While this approach has proven extremely useful for peptide discovery, nontargeted HPLC−MS preferentially identifies the most prevalent peptides, which are not necessarily the most immunogenic.[21] In recent years computational algorithms have been developed to predict which peptides in a protein are likely to bind specific HLA molecules.[22−26] These algorithms, when combined with the significant advances in genomics and computational biology, can be used to predict the relatively small number of antigenic peptides in tumor extracts that are likely immunogenic and cancer-specific because they are produced as a result of cancer-specific processes such as somatic gene mutations, fusions, overexpression, and alternative splicing.[27,28]

By employing a computationally predictive cancer-antigen discovery approach, targeted MS methodologies aimed at detecting cancer-specific peptide antigens would facilitate the discovery of high-value cancer peptide antigens. In this study, a targeted antigen-discovery strategy employing DIMS−MS/MS was used to identify known cancer-associated antigenic peptides from a human leukemia cell line without using HPLC.

EXPERIMENTAL SECTION

Model Peptide Pool

A panel of 95 "Flashpure" peptides (New England Peptide, Gardner MA) that had been computationally predicted to bind with high affinity to HLA-A*0201 (Supplementary Table S-1) were dissolved in 100% DMSO to a concentration of 20 mM and subsequently diluted to 1 μM using 50/49.9/0.1 ACN/H_2O/FA (V/V/V) (Sigma-Aldrich, St. Louis, MO) (Supplementary Table S-1). To create a peptide pool, 94 of the 20 mM peptide solutions in DMSO were combined in equal volumes and diluted to a final concentration of 1 μM of each peptide in 50/49.9/0.1 ACN/H_2O/FA (V/V/V). The 95th peptide, GLR (amino acid sequence FLSSANEHL), was further diluted using 50/49.9/0.1 ACN/H_2O/FA (V/V/V) and spiked into the 94 peptide pool to make 1 μM, 100 nM, 10 nM, 100 pM, 10 pM, and 1 pM concentrations of GLR peptide solutions.

Leukemia Cell Line Derived Peptide Mixture

The U937 leukemia cell line stably transfected with HLA-A*0201 (called U937.A2) were grown under sterile conditions at 37 °C with 5% CO_2 in a medium consisting of RPMI 1640 supplemented with 10% heat inactivated (56 °C for 30 min) fetal bovine serum (FBS), 1% penicillin−streptomycin, and 1% L-glutamine.[29] Four liters of U937.A2 cell culture suspension was incubated until the live cell density reached ~7.5×10^5 cells/mL. The cell suspension (approximately 2 to 3×10^9 U937.A2 cells) was centrifuged at 4 °C for 30 min at 1250 rpm to obtain a cell pellet, and then the pelleted cells were lysed in 20 mM Tris-HCl, pH 8, 150 mM NaCl, 1% (mass/volume) 3-[(3-cholamidopropyl) dimethylammonio]-1-propanesulfonate (CHAPS), 1 mM (phenylmethylsulfonyl fluoride), 10 μg/mL pepstatin, 5 μg/mL aprotinin, and 10 μg/mL leupeptin (Sigma-Aldrich, St. Louis, MO). The mixture was gently rocked in a laboratory shaker for 15 min at 4 °C to break up the cells. The cell lysate was subjected to ultracentrifugation at 40,000 rpm for 1 h to remove cell debris.[30] All protein loading and elution steps were then performed using a Chemyx Fusion 100 syringe pump (Stafford, TX). The cell pellet consisted of ~2×10^9 cells of U937.A2 with each cell estimated to have ~10,000 HLA-A*0201 molecules.[31,32] For efficient isolation of nearly all the HLA-A*0201 molecules in the lysate, 100× excess molecules (3.3×10^{-9} moles) of the anti-HLA-A*0201 antibody, BB7.2, were introduced into a 5 mL GE Healthcare HiTRAP recombinant protein A column (Chicago, IL) for the immobilization. The BB7.2 antibody molecules were reconstituted in 200 mM Tris HCl (pH 8) (Sigma-Aldrich, St. Louis, MO). For effective antibody immobilization, first, the column was washed with 50 mM Tris (pH 8) for 5 min at 1 mL/min flow rate. Then, the reconstituted BB7.2 solution (1 mL) was injected into the column at 0.2 mL/min flow rate for 5 min. Excess antibody was washed out using 200 mM Tris HCl (pH 8) at 1 mL/min for 5 min.

The HLA-A*0201/peptide complex containing supernatant was introduced into the BB7.2 antibody immobilized column at 1 mL/min for immunoaffinity capture of HLA-A*0201/peptide complexes. Then, the column was washed using 50 mM Tris (pH 8) solution at 0.5 mL/min for 5 min to remove excess cell lysate in the column. Finally, 0.2 M acetic acid solution (pH 3) was introduced at a flow rate of 0.5 mL/min for 10 min to elute the immobilized HLA-A*0201/peptide complexes from the column surface. The output was collected into 1.5 mL low-protein binding microcentrifuge tubes. Glacial acetic acid (17.5 M original) was added to the eluate to increase the acetic acid percentage to 10% to dissociate the HLA-A*0201 from the peptides. Finally, the peptides were separated from the high molecular weight proteins by centrifugation at 3220 rpm in 4 °C for 40 min on an Amicon Ultra-3 kDa device (Millipore, Billerica, MA). The peptide extract was lyophilized for ~8 h at 40 °C. The lyophilized peptide samples were stored in −80 °C until they were analyzed by DIMS−MS/MS.

Mass Spectrometry

A Bruker HCT ion trap mass spectrometer was used for these experiments. The lyophilized samples obtained from the cell line were reconstituted for electrospray ionization (ESI) in 60 μL of 50/49.9/0.1 ACN/H_2O/FA (V/V/V) and were directly infused for electrospray ionization (ESI) at a flow rate of 2 μL/min. The scan rate was 26,000 (m/z)/s for all mass spectra. All MS/MS spectra represent an average of ten to 11 spectra.

Differential Ion Mobility Spectrometry

The ESI emitter was held at ground potential, and a voltage of −4.25 kV was applied to the custom built planar DIMS electrode assembly and housing (Figure 1). The two parallel stainless steel 4 × 10 mm electrodes are separated by a 0.3 mm gap. The assembly slides onto the glass transfer capillary of the

dx.doi.org/10.1021/pr500527c | J. Proteome Res. 2014, 13, 4356−4362

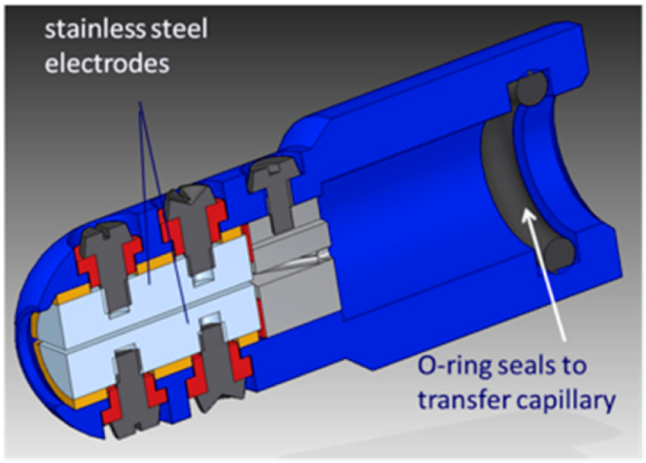

Figure 1. AutoCAD drawing of DIMS assembly.

source region of the mass spectrometer. A housing is then oriented around the assembly to reroute the desolvation gas, which also serves as the carrier gas through the device. The temperature of the desolvation gas is set to 300 °C in the instrument software. The residence time for ions in the device is 0.2 ms.

Ideally, a square wave should be used for DIMS, alternating between low and high electric fields of opposing polarity. However, because of the high power requirements of high-voltage, high-frequency square waves, most DIMS waveforms are bisinusoidal, approximating a square wave (Figure 2).[33] In

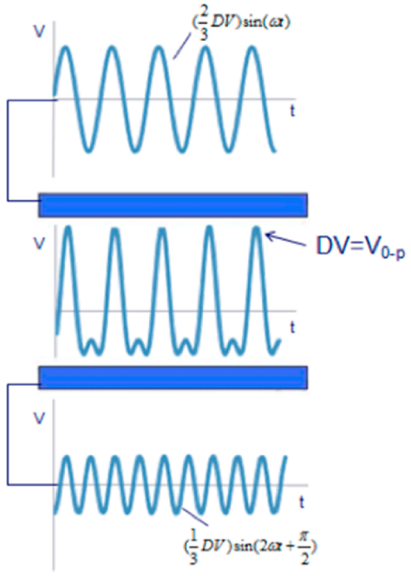

Figure 2. Simplified schematic of the addition of sinusoidal waves across the gap to form a bisinusoidal waveform.

these experiments the waveform generator output a sinusoidal wave at 2 MHz and a lower amplitude sinusoidal wave at 4 MHz, phase shifted about 90°. Each sinusoidal wave is applied to one of the electrodes, and thus, they are capacitatively summed across the gap to form the bisinusoidal DIMS waveform at frequency of 2 MHz.[34] DIMS spectra were acquired by scanning the CV using a LabVIEW program linked to the instrument control software. Ten mass spectra were averaged for each CV in the DIMS spectra. A static CV for the filter mode can also be selected with the LabVIEW program. The MS/MS spectra shown for the filter mode were averaged for 1 min at the static CV.

RESULTS AND DISCUSSION

Spiked Peptide in a Model Peptide Pool

The model peptide pool that was generated was intended to simulate a complex mixture of very similar peptides (by molecular weight, hydrophobicity, and sequence) such as that which would be seen in a collection of antigen peptides obtained from a biological source. A DIMS scan of a solution of the pure "target" peptide, protonated GLR (amino acid sequence = FLSSANEHL), was performed to determine the optimum CV for selection of this peptide. The DIMS spectrum is shown in Figure 3. At a DV of 1200 V, the optimum CV was determined to be 6.5 V.

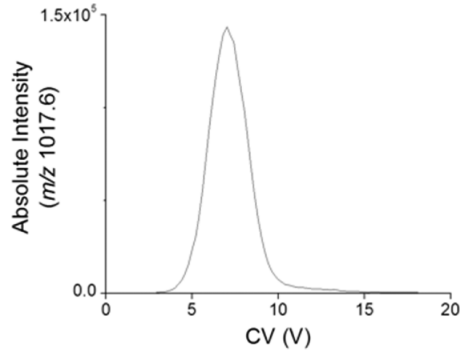

Figure 3. DIMS scan of protonated FLSSANEHL (also called GLR m/z 1017.5) at a DV of 1200 V.

The MS/MS spectrum obtained for pure GLR (m/z 1017.5) was compared to that obtained for the mixture of 94 peptides (Figure 4a). Without GLR spiked into the mixture, none of the product ions observed from pure GLR were present (Figure 4b). The GLR peptide was spiked into the 94-peptide pool at concentrations ranging from 1 μM to 1 pM. For each solution the MS/MS spectrum at the mass-to-charge ratio of the target protonated GLR peptide was taken with and without DIMS active. The five most intense product ions observed in the MS/MS spectrum of pure GLR, $[M + H - H_2O]^+$, $[M + H - NH_3]^+$, $[M + H - H_2O - NH_3]^+$, b_8, and b_8-NH_3 were used to evaluate whether GLR was detectable at each concentration. With 1 pM GLR spiked into the mixture, two of the five product ions were observable at a signal-to-background ratio greater than 3, where background is defined as the signal obtained for the mixture without GLR spiked in. However, the ratio of these product ions deviated too much from the reference spectrum to consider the peptide to be detected at this concentration. With 10 pM GLR spiked into the mixture, all five of the product ions were observable, with a contaminant ion present that was observed without GLR (Figure 4c). Without DIMS, none of the product ions observed at greater than 5% relative intensity match those observed from MS/MS of protonated GLR (Figure 4d). Using the detection of five product ions as indicative of the presence of the target ion (in typical biomarker detection, only two product ions are used to confirm the presence of an analyte), a comparison of the detection of GLR in the peptide mix with and without DIMS was made (Figure 5a,b). The red line represents the signal

dx.doi.org/10.1021/pr500527c | J. Proteome Res. 2014, 13, 4356−4362

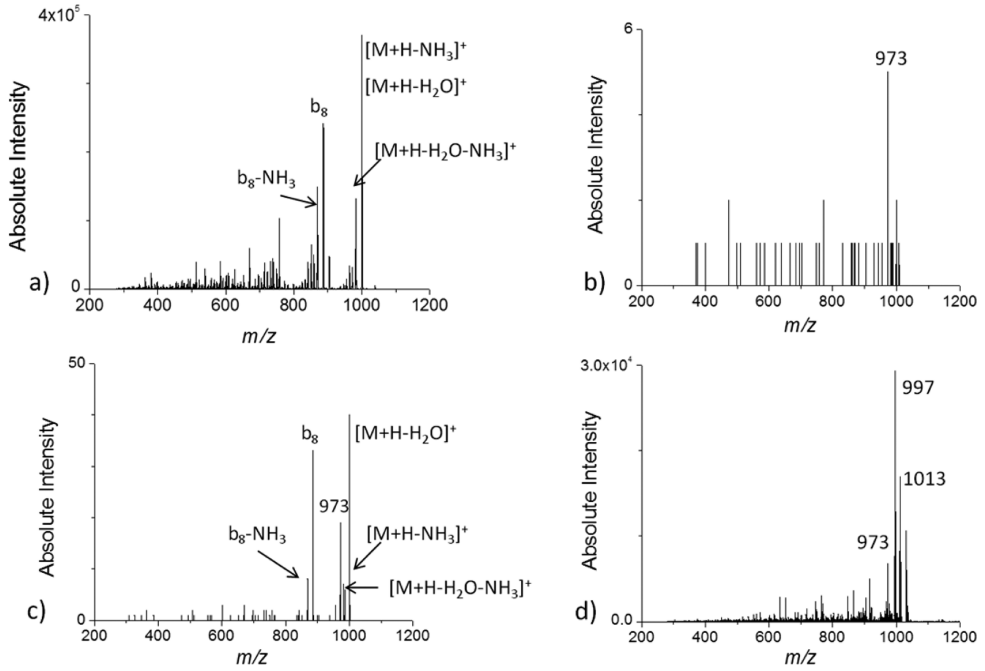

Figure 4. MS/MS of protonated FLSSANEHL (GLR), where panel a was obtained for 10 μM FLSSANEHL in 50/49.9/0.1 acetonitrile/water/formic acid, panels b and c were obtained with DIMS at a DV of 1200 V and a CV of 6.5 V, where panel b was obtained for a mixture of 94 peptides without FLSSANEHL added, and panel c was obtained for the same mixture of 94 peptides, but with 10 pM FLSSANEHL in the mixture, and panel d was obtained without DIMS for the mixture of 94 peptides with 10 pM FLSSANEHL.

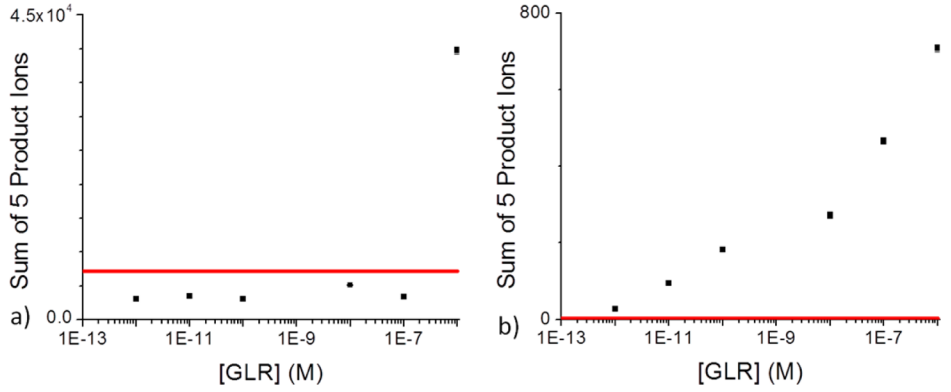

Figure 5. Sum of the intensities of the five most intense product ions observed from MS/MS of protonated FLSSANEHL as a function of the concentration of FLSSANEHL (GLR) in the mixture of 94 peptides, where panel a is without DIMS and panel b is with DIMS under the optimum conditions for the selection of protonated GLR. The red line indicates the signal intensity at which the signal-to-background ratio is 3, where background is defined as the signal obtained for the mixture of 94 peptides without GLR spiked in.

intensity at which the signal-to-background ratio is equal to 3. In this model peptide pool, the target antigen was readily detected at a concentration of 10 pM in a mixture of 94 other peptides possessing similar chemical properties. Each MS/MS scan was obtained using a volume of ~2 μL; so the system is able to identify peptides at the low attomole level. This level of sensitivity (20 amol = 1.2 × 10^7 molecules) is important when considering applying this technique for use in human cancer samples. In the case of acute leukemia, most patient samples have ~1 × 10^7 leukemia cells per mL of whole blood with each cell possessing ~10,000 HLA molecules. A routine blood draw of 10 mL would therefore be expected to yield 1 × 10^{12} peptides, present at various frequencies, making the application of DIMS−MS/MS for leukemia antigen discovery feasible in most clinical samples.[31,32] In solid tumors, a 1 cm^3 sample contains ~1 × 10^8 cells; so again DIMS−MS/MS has the potential for use in readily accessible clinical specimens.[35]

Identification of a Known Cancer Associated Antigen, CG1, Using DIMS−MS/MS

A significant problem in cancer immunology is the identification of cancer-specific peptide antigens, which can then be developed into cancer immunotherapeutics, such as vaccines.[12,36,37] To demonstrate how DIMS−MS/MS could be applied to this problem, the device was used to detect three known cancer antigens from a model leukemia cell line, U937.A2. The three peptide antigens targeted, CG1 (FLLPTGAEA), UNC-CDK4-1 (ALTPVVVTL), and UNC-ANKRD17-1 (LLIERGASL), are (1) derived from proteins that are overexpressed or aberrantly processed in human acute myeloid leukemia (AML), (2) computationally predicted to bind with high affinity to HLA-A*0201 (the most common

dx.doi.org/10.1021/pr500527c | J. Proteome Res. 2014, 13, 4356−4362

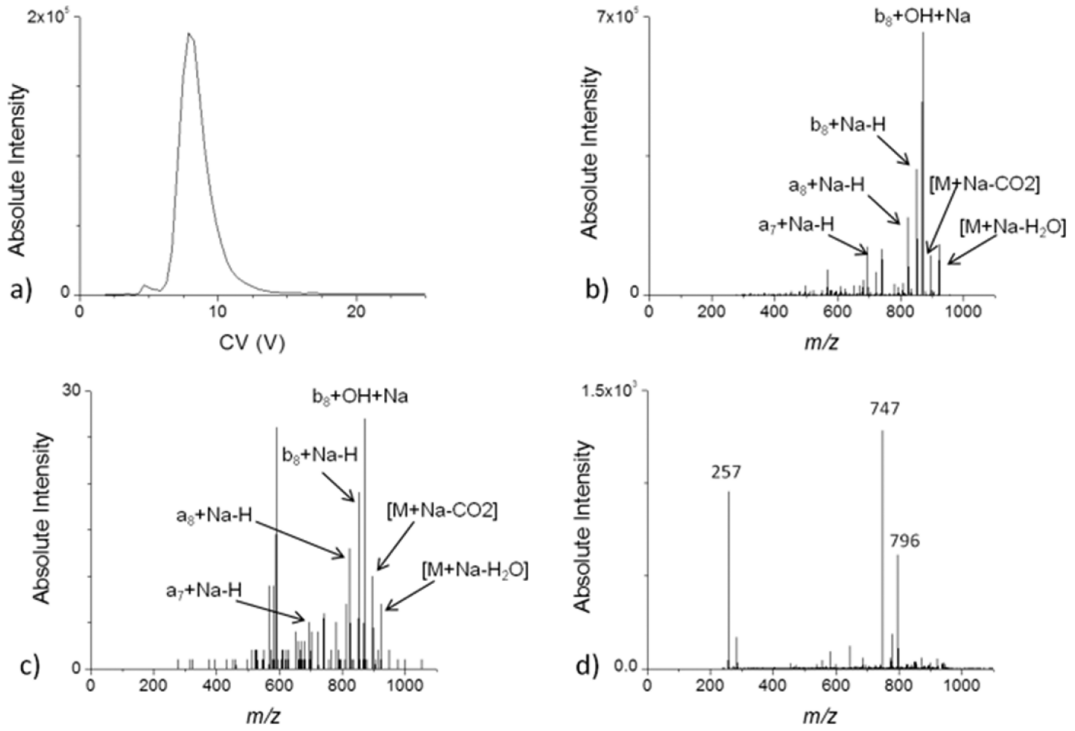

Figure 6. (a) DIMS scan of sodiated FLLPTGAEA (m/z 940.6) and MS/MS obtained for sodiated FLLPTGAEA, where panel b was obtained for 10 μM FLLPTGAEA in 50/49.9/0.1 acetonitrile/water/formic acid, panel c was obtained for the peptide cell extract with DIMS with a DV of 1200 V and a CV of 7.8 V, and panel d was obtained for the peptide cell extract without DIMS.

HLA type), and (3) have been previously shown to be presented by U937.A2 cells.[23,25,38]

The optimum CV to select for sodiated CG1 (FLLPTGAEA + Na^+, m/z 940.4) at a DV of 1200 V was determined to be 7.8 V from a DIMS scan of the pure peptide (Figure 6a). Note that, rather than the analysis being performed with the protonated peptide, the sodiated peptide was used because there was greater sensitivity with the latter. The sodiated peptide would likely not be seen in an LC/MS experiment because the LC effectively "desalts" the sample, and there would be no sodium present in the solvent to effect ionization when the peptide eluted. The MS/MS of the pure CG1 peptide is shown in Figure 6b. MS/MS of sodiated peptides has been extensively studied, and in general, the fragmentation efficiency is as good or better than that observed for protonated peptides.[39,40] With DIMS, the peptide cell extract MS/MS spectrum of m/z 940.4 exhibited five product ions that matched the MS/MS of the pure peptide as well as a contaminant peak (Figure 6c). Without DIMS, none of the product ions observed at greater than 5% relative intensity match those observed from the MS/MS of sodiated CG1 (Figure 6d).

This approach was used for two other previously confirmed antigen peptides UNC-CDK4-1 (ALTPVVVTL) and UNC-ANKRD17-1 (LLIERGASL).[38] After determining the optimum CVs for UNC-CDK4-1 and UNC-ANKRD17-1, the same discovery experiment was performed as described above. In the case of UNC-CDK4-1, four identifiable product ions could be detected in the MS/MS with DIMS active and with DIMS transparent (Supplementary Figure S-1 a-c). For UNC-ANKRD17-1, one identifiable product ion could be assigned on the MS/MS with DIMS active, and no product ions could be identified without DIMS (Supplementary Figure S-2 a-c). With one observed product ion, we believe we have detected this peptide but cannot confirm its detection due to the lack of additional product ions and inability to perform MS^3 due to low ion intensity. In all 3 peptides tested, DIMS−MS/MS performed as well or better than MS/MS alone. Multiple product ions from the MS/MS spectra could be identified with DIMS active for both CG1 and UNC-CDK4-1.

■ CONCLUSIONS

Many human tumors are susceptible to T-cell mediated killing; however, to avoid off-target toxicity, T-cell immunotherapeutics such as vaccines or adoptive cellular therapy must target specific cancer-associated antigens.[12,36,41−43] Nontargeted HPLC−MS has typically been used to identify these antigens.[15−17,19,20] In this work we demonstrate that cancer antigens can be identified using a targeted MS approach, aimed at identifying specific antigens, and that DIMS significantly improved our ability to confirm the presence of antigens by improving the signal-to-noise of the MS experiments.

Cancer antigen discovery using nontargeted MS methods have typically required extremely large cell populations of >1 × 10^9 cells per analysis, which makes analysis of most clinical samples impossible.[19] While we originally expanded >1 × 10^9 U937.A2 cells, the isolated peptides were divided into 10 aliquots so that the antigen discovery experiments were performed on peptides from ∼1 × 10^8 cells, a number of cells that can be obtained in many more clinical specimens, particularly AML samples.[35] The ability to detect antigens using these small quantities of cellular material is a result of our targeted approach to antigen discovery and the improved signal-to-noise of the DIMS device, which we observed in all experiments, when used in a targeted antigen discovery method.

Over the past two decades, computational algorithms have greatly enhanced our ability to predict cancer antigens.[22−26]

dx.doi.org/10.1021/pr500527c | J. Proteome Res. 2014, 13, 4356−4362

With this advancement, targeted MS approaches, as described in this article, can now be used to screen for and identify high value cancer antigens. This approach is particularly exciting given the dramatic expansion of cancer genome sequencing.[44] With these types of genomic data, it is possible to probe patient tumor genomes and predict candidate antigens that result from genetic lesions in the tumor itself.[27] DIMS−MS/MS could then be applied to specific patient samples to confirm or deny the presence of the predicted antigen, which could lead to more informed decisions regarding possible cancer immunotherapies. Modifications to our current device could include further optimization of the DIMS electrodes to improve focusing of the ion stream in the DIMS prior to entry into the MS and the use of nanospray ionization.

■ ASSOCIATED CONTENT

Supporting Information

Peptide sequences, molecular weights, and predicted HLA-A*0201 binding affinities for the 95 peptides in the peptide pool. MS/MS spectra with and without DIMS for two of the previously identified cancer antigens in the cell extract (UNC-CDK4-1 and UNC-ANKRD17-1). This material is available free of charge via the Internet at http://pubs.acs.org.

■ AUTHOR INFORMATION

Corresponding Author

*(P.M.A.) E-mail: parmiste@med.unc.edu.

Present Address

§(U.D.) Entegris, Inc., 129 Concord Road, Billerica, Massachusetts 01821, United States.

Author Contributions

The manuscript was written through contributions of all authors. All authors have given approval to the final version of the manuscript.

Notes

The authors declare the following competing financial interest(s): Bruker Daltonics does have a license to some of the DIMS related technology developed in the Glish laboratory.

■ ACKNOWLEDGMENTS

The HLA-A*0201 transfected U937 cell line (U937.A2) was a generous gift of Dr. Greg Lizée at M.D. Anderson Cancer Center, Houston TX. Salary support for P.M.A. was provided through NIH K08 HL113594.

■ REFERENCES

(1) Hatsis, P.; Valaskovic, G.; Wu, J. T. Online nanoelectrospray/high-field asymmetric waveform ion mobility spectrometry as a potential tool for discovery pharmaceutical bioanalysis. *Rapid Commun. Mass Spectrom.* **2009**, *23*, 3736−42.

(2) Kolakowski, B. M.; Mester, Z. Review of applications of high-field asymmetric waveform ion mobility spectrometry (FAIMS) and differential mobility spectrometry (DMS). *Analyst* **2007**, *132*, 842−64.

(3) Xia, Y. Q.; Wu, S. T.; Jemal, M. LC-FAIMS-MS/MS for quantification of a peptide in plasma and evaluation of FAIMS global selectivity from plasma components. *Anal. Chem.* **2008**, *80*, 7137−43.

(4) Eiceman, G.; Karpas, Z. *Ion Mobility Spectrometry*; CRC Press: Boca Raton, FL, 2005.

(5) Mason, E. A.; McDaniel, E. W. *Transport Properties of Ions in Gases*; John Wiley & Sons, Inc.: New York, 1988.

(6) Hinrichs, C. S.; Restifo, N. P. Reassessing target antigens for adoptive T-cell therapy. *Nat. Biotechnol.* **2013**, *31*, 999−1008.

(7) Jensen, P. E. Recent advances in antigen processing and presentation. *Nat. Immunol* **2007**, *8*, 1041−8.

(8) Neefjes, J.; Jongsma, M. L.; Paul, P.; Bakke, O. Towards a systems understanding of MHC class I and MHC class II antigen presentation. *Nat. Rev. Immunol.* **2011**, *11*, 823−36.

(9) Phan, G. Q.; Rosenberg, S. A. Adoptive cell transfer for patients with metastatic melanoma: the potential and promise of cancer immunotherapy. *Cancer Control* **2013**, *20*, 289−97.

(10) George, S.; Pili, R.; Carducci, M. A.; Kim, J. J. Role of immunotherapy for renal cell cancer in 2011. *J. Natl. Compr. Cancer Network* **2011**, *9*, 1011−8.

(11) Michael, A.; Relph, K.; Annels, N.; Pandha, H. Prostate cancer vaccines. *Expert Rev. Vaccines* **2013**, *12*, 253−62.

(12) Rezvani, K.; de Lavallade, H. Vaccination strategies in lymphomas and leukaemias: recent progress. *Drugs* **2011**, *71*, 1659−74.

(13) Linette, G. P.; Stadtmauer, E. A.; Maus, M. V.; et al. Cardiovascular toxicity and titin cross-reactivity of affinity-enhanced T cells in myeloma and melanoma. *Blood* **2013**, *122*, 863−71.

(14) Warren, E. H.; Fujii, N.; Akatsuka, Y.; et al. Therapy of relapsed leukemia after allogeneic hematopoietic cell transplantation with T cells specific for minor histocompatibility antigens. *Blood* **2010**, *115*, 3869−78.

(15) den Haan, J. M.; Meadows, L. M.; Wang, W.; et al. The minor histocompatibility antigen HA-1: a diallelic gene with a single amino acid polymorphism. *Science* **1998**, *279*, 1054−7.

(16) den Haan, J. M.; Sherman, N. E.; Blokland, E.; et al. Identification of a graft versus host disease-associated human minor histocompatibility antigen. *Science* **1995**, *268*, 1476−80.

(17) Fortier, M. H.; Caron, E.; Hardy, M. P.; et al. The MHC class I peptide repertoire is molded by the transcriptome. *J. Exp. Med.* **2008**, *205*, 595−610.

(18) Mohammed, F.; Cobbold, M.; Zarling, A. L.; et al. Phosphorylation-dependent interaction between antigenic peptides and MHC class I: a molecular basis for the presentation of transformed self. *Nat. Immunol.* **2008**, *9*, 1236−43.

(19) Papadopoulos, K. P.; Suciu-Foca, N.; Hesdorffer, C. S.; Tugulea, S.; Maffei, A.; Harris, P. E. Naturally processed tissue- and differentiation stage-specific autologous peptides bound by HLA class I and II molecules of chronic myeloid leukemia blasts. *Blood* **1997**, *90*, 4938−46.

(20) van Bergen, C. A.; Kester, M. G.; Jedema, I.; et al. Multiple myeloma-reactive T cells recognize an activation-induced minor histocompatibility antigen encoded by the ATP-dependent interferon-responsive (ADIR) gene. *Blood* **2007**, *109*, 4089−96.

(21) Gallegos, A. M.; Bevan, M. J. Central tolerance: good but imperfect. *Immunol. Rev.* **2006**, *209*, 290−6.

(22) Hoof, I.; Peters, B.; Sidney, J.; et al. NetMHCpan, a method for MHC class I binding prediction beyond humans. *Immunogenetics* **2009**, *61*, 1−13.

(23) Lundegaard, C.; Lamberth, K.; Harndahl, M.; Buus, S.; Lund, O.; Nielsen, M. NetMHC-3.0: accurate web accessible predictions of human, mouse and monkey MHC class I affinities for peptides of length 8−11. *Nucleic Acids Res.* **2008**, *36*, W509−12.

(24) Nielsen, M.; Lundegaard, C.; Lund, O.; Kesmir, C. The role of the proteasome in generating cytotoxic T-cell epitopes: insights obtained from improved predictions of proteasomal cleavage. *Immunogenetics* **2005**, *57*, 33−41.

(25) Nielsen, M.; Lundegaard, C.; Worning, P.; et al. Reliable prediction of T-cell epitopes using neural networks with novel sequence representations. *Protein Sci.* **2003**, *12*, 1007−17.

(26) Rammensee, H. G.; Bachmann, J.; Emmerich, N. N.; Bachor, O. A.; Stevanovic, S. SYFPEITHI: database for MHC ligands and peptide motifs. *Immunogenetics* **1999**, *50*, 213−9.

(27) Robbins, P. F.; Lu, Y. C.; El-Gamil, M.; et al. Mining exomic sequencing data to identify mutated antigens recognized by adoptively transferred tumor-reactive T cells. *Nat. Med.* **2013**, *19*, 747−52.

(28) Pang, C. N.; Tay, A. P.; Aya, C. Tools to covisualize and coanalyze proteomic data with genomes and transcriptomes: validation

of genes and alternative mRNA splicing. *J. Proteome Res.* **2014**, *13*, 84−98.
(29) Rodriguez-Cruz, T. G.; Liu, S.; Khalili, J. S.; et al. Natural splice variant of MHC class I cytoplasmic tail enhances dendritic cell-induced CD8+ T-cell responses and boosts anti-tumor immunity. *PLoS One* **2011**, *6*, e22939.
(30) Zhang, M.; Sukhumalchandra, P.; Enyenihi, A. A.; et al. A novel HLA-A*0201 restricted peptide derived from cathepsin G Is an effective immunotherapeutic target in acute myeloid leukemia. *Clin. Cancer Res.* **2013**, *19*, 247−57.
(31) Princiotta, M. F.; Finzi, D.; Qian, S. B.; et al. Quantitating protein synthesis, degradation, and endogenous antigen processing. *Immunity* **2003**, *18*, 343−54.
(32) Yewdell, J. W.; Reits, E.; Neefjes, J. Making sense of mass destruction: quantitating MHC class I antigen presentation. *Nat. Rev. Immunol.* **2003**, *3*, 952−61.
(33) Krylov, E. V.; Coy, S. L.; Vandermey, J.; Schneider, B. B.; Covey, T. R.; Nazarov, E. G. Selection and generation of waveforms for differential mobility spectrometry. *Rev. Sci. Instrum.* **2010**, *81*, 024101.
(34) Isenberg, S. L.; Armistead, P. M.; Glish, G. L. Optimization of peptide separations by differential ion mobility spectrometry. *J. Am. Soc. Mass Spectrom.* **2014**, *25*, 1592−9.
(35) Del Monte, U. Does the cell number 10(9) still really fit one gram of tumor tissue? *Cell Cycle* **2009**, *8*, 505−6.
(36) Mittendorf, E. A.; Clifton, G. T.; Holmes, J. P.; et al. Clinical trial results of the HER-2/neu (E75) vaccine to prevent breast cancer recurrence in high-risk patients: from US Military Cancer Institute Clinical Trials Group Study I-01 and I-02. *Cancer* **2012**, *118*, 2594−602.
(37) Rezvani, K.; Yong, A. S.; Mielke, S.; et al. Leukemia-associated antigen-specific T-cell responses following combined PR1 and WT1 peptide vaccination in patients with myeloid malignancies. *Blood* **2008**, *111*, 236−42.
(38) Hunsucker, S. A.; McGary, C. S.; Vincent, B. G.; et al. Mapping of Antigen-Specific T-Cell Receptor Sequences to T-Cell Receptor Repertoires Measures Antigen-Driven, Clonal T-cell Expansion. *Cancer Immunol. Res.* **2014**, under revision.
(39) Lin, T.; Glish, G. L. C-terminal peptide sequencing via multistage mass spectrometry. *Anal. Chem.* **1998**, *70*, 5162−5.
(40) Lin, T.; Payne, A. H.; Glish, G. L. Dissociation pathways of alkali-cationized peptides: opportunities for C-terminal peptide sequencing. *J. Am. Soc. Mass Spectrom.* **2001**, *12*, 497−504.
(41) Chapuis, A. G.; Ragnarsson, G. B.; Nguyen, H. N.; et al. Transferred WT1-reactive CD8+ T cells can mediate antileukemic activity and persist in post-transplant patients. *Sci. Transl. Med.* **2013**, *5*, 174ra27.
(42) Meij, P.; Jedema, I.; van der Hoorn, M. A.; et al. Generation and administration of HA-1-specific T-cell lines for the treatment of patients with relapsed leukemia after allogeneic stem cell transplantation: a pilot study. *Haematologica* **2012**, *97*, 1205−8.
(43) Rezvani, K.; Yong, A. S.; Mielke, S.; et al. Repeated PR1 and WT1 peptide vaccination in Montanide-adjuvant fails to induce sustained high-avidity, epitope-specific CD8+ T cells in myeloid malignancies. *Haematologica* **2011**, *96*, 432−40.
(44) Genomic and epigenomic landscapes of adult de novo acute myeloid leukemia. *N. Engl. J. Med.* **2013**;*368*:2059−74.